

# Paramagnetic Meissner effect depending on superconducting thickness in Co/Nb multilayers

S. F. Lee, J. J. Liang, T. M. Chuang, S. Y. Huang, J. H. Kuo, and Y. D. Yao

*Institute of Physics, Academia Sinica,*

*Taipei, Taiwan 115, Republic of China*

(Dated: November 9, 2018)

## Abstract

Paramagnetic Meissner Effect (PME) was observed in Co/Nb/Co trilayers and multilayers. Measurements of the response to perpendicular external field near the superconducting transition temperature were carried out for various Nb thicknesses. PME was found only when layer thickness is no smaller than penetration depth of Nb. A classical flux compression model [Koshelev and Larkin, Phys. Rev. B **52**, 13559 (1995)] was used to explain our data. We inferred that the penetration depth was a critical length, below which superconducting current density became too small and the PME could not be achieved.

PACS numbers: 74.60.Ec, 74.25.Ha, 74.60.Ge, 74.62.Bf

## I. INTRODUCTION

Meissner effect is the intrinsic diamagnetic response of superconductivity to external magnetic field. Instead, Paramagnetic Meissner effect (PME), also known as Wohleben effect<sup>1</sup> refers to weak paramagnetic signals observed in some field-cooled superconductive samples. It was first observed in high  $T_C$  ceramic samples and later on in Nb foils, a conventional superconductor (S). Although the experimental observations are similar, the PME in high  $T_C$  cuprate and in BCS superconductors are attributed to different underlying physics (see below). What is common is that only certain samples show PME. Surface treatment of the Nb samples could make this effect disappear.<sup>2,3</sup> Ferromagnetic (F) materials can suppress Cooper pairs very efficiently due to the exchange field. This proximity effect reduces  $T_C$  near the S/F interface. Since the pioneer work of Hauser *et al.*,<sup>4</sup> it is well-known that ferromagnetic materials suppress  $T_C$  of adjacent superconducting films much stronger than non-magnetic materials. Experimental data on Fe/Pb/Fe trilayers<sup>5</sup> and on Nb/Fe multilayers<sup>6</sup> showed that as S layer thickness decreased,  $T_C$  dropped to zero at critical thickness 70 nm and 32 nm, respectively. In contrast, in Nb/Cu multilayers,<sup>7</sup> superconductivity persisted down to Nb thickness less than 5 nm. Thus, Co modifies the interface properties much more pronounced than non-magnetic materials. We thus focus on the field-cooled magnetic moments in Co/Nb multilayers to study the interface effect and the role of penetration depth.

Paramagnetic field-cooled magnetization (FCM) for high  $T_C$  cuprate samples was first reported by Svelindh *et al.*<sup>8</sup> using a non-commercial SQUID magnetometer, in which the samples were kept stationary during measurements. Zero-field-cooled magnetization of those samples showed usual Meissner effect, but FCM in small external fields were paramagnetic. The PME signal decreased with increasing external field and became usual diamagnetic one for large field.

A systematic study of PME was later reported by Wohleben and coworkers.<sup>1</sup> They found several melt processed  $\text{Bi}_2\text{Sr}_2\text{CaCu}_2\text{O}_8$  samples showed PME when field is  $\leq 0.5$  Oe. They invoked “ $\pi$ -junction” as a possible origin of the PME, which induced negative spontaneous supercurrents across weak links of crystalline structures.

Results similar to the PME in High  $T_C$  materials on Nb disks with perpendicular field were later reported by Thompson *et al.*<sup>2</sup> They showed PME disappeared by various surface treatments and suggested that the surface layers having strong flux pinning sites together

with sample orientation and geometry were responsible for the observation of PME. The same conclusion was also reached by Kostic *et al.*<sup>3</sup> They showed that samples exhibit PME have surface  $T_C$  different from their bulk values. Strong and reversible PME was reported to exist up to 2000 Oe by Pust *et al.*<sup>9</sup> Since the observed effect is reversible, flux motion was excluded from being responsible. However, Terentiev *et al.*<sup>10</sup> reported that non-uniform applied fields or vortex dynamics play important roles in the PME in Nb films less than 100 nm thick. Geim *et al.*<sup>11</sup> measured micrometer size Nb and Al disks by a ballistic Hall magnetometer with detection loops  $\sim 1\mu\text{m}^2$ , which utilized two-dimensional electron gas in semiconductor heterostructure. They found PME to be an oscillating function of external field and concluded that the PME was related to surface superconductivity.

Different theoretical models for the PME were proposed. One explanation was Josephson loops with a spontaneous negative critical current, i.e.,  $\pi$ -junctions caused by impurities or grain boundary scattering. PME was also used as an evidence for d-wave symmetry in High  $T_C$  materials.<sup>12</sup> Since only in certain but not all samples can PME be found, it is most likely caused by surface or micro-structural defects rather than being an intrinsic property. To explain the PME in Nb, a flux compression model was demonstrated to result in paramagnetic moment because of inhomogeneous superconducting transition or the surface layer having a higher  $T_C$  than the bulk material.<sup>13</sup> It treated current and field distributions for the cases of complete and partial Bean state. Superconducting currents at the sample surface forming ‘giant vortexes’ was raised as another model.<sup>14</sup> From the self-consistent solution to the Ginzburg-Landau equations, it was proved that a giant vortex state at the surface can be formed when S is field-cooled at  $H_{c3}$ , the surface critical field. This state has an S order parameter with a fixed orbital quantum number  $L$ . When temperature decreases further, flux can be trapped and compressed into a giant vortex state with paramagnetic signal.

## II. EXPERIMENTAL METHODS

We fabricated several series of Nb films, Nb/Co trilayers and multilayer samples by dc sputtering onto Si (100) substrates. Samples with  $2\mu\text{m}$  line-width and  $40\mu\text{m}$  in length were also fabricated by lithography technique to measure critical currents. Base pressure in the vacuum chamber is  $2 \times 10^{-7}$  Torr or better. Deposition was made under 1 mTorr Ar gas,

with 0.05 nm/s rate for Co and 0.12 nm/s for Nb. Twelve samples can be fabricated in the same run.<sup>15,16</sup> As the Nb target became thinner, the deposition rate increased slightly to 0.15nm/s. Prolong the pre-sputtering time between ignition of plasma and start of deposition of Nb improved the sample quality, as pointed out by Muhge et al.<sup>17</sup> In this paper, we concentrate on three Nb thicknesses: 240nm, 80nm, and 30nm, with all samples having the same total Nb thickness in each series. Magnetic measurements at low temperatures were performed by a commercial SQUID magnetometer. Data presented here are measured with field perpendicular to layer plane. We have shown that the S penetration depth in our Nb/Co multilayers was about 30 to 40nm at each interface.<sup>16</sup> The average saturation moment of Co decreased only when nominal thickness was less than 1.5nm. Nb layers with thickness of 30nm sandwiched between Co was just above the critical thickness, below which no S transition could be found.<sup>18</sup>

As already pointed out,<sup>19</sup> S samples measured with commercial SQUID magnetometers showed artifact because the superconducting magnet has inevitably non-uniform field. Indeed, we reached the same conclusion that S signals depended on the sample position while cooling through  $T_C$ , on the scan length in the superconducting magnet, and on the field uniformity etc. Since the resulting signal, voltage versus position, was no longer symmetrical with respect to the magnet center, commercial fitting routine in the automated software sequence might sometimes pick the wrong maximum and give a wrong sign to the measured moment. We measured our sample with the samples kept stationary and with a temperature sweeping rate of 0.05K/min. Signals were normalized to a Pb foil sample measured below  $T_C$  with a 4-cm scan. Applied field was calibrated also by the Pb foil because of its large diamagnetic response. Moment versus field above  $T_C$  was also measured by standard 4-cm scan with the SQUID voltage response monitored closely. Asymmetric curves were frequently observed, indicating non-ideal dipole response, due to the perpendicular direction was a hard axis. In cgs unit, the volume susceptibility for complete Meissner effect was  $-1/4\pi$ . The small total S volume of the samples,  $\sim 3\text{mm} \times 3\text{mm} \times 240\text{nm}$ , would have made the signal to be detected below the SQUID limit. This was compensated by the demagnetization factor,  $d$ , of the perpendicular geometry. Taking into account this factor, magnetization per unit volume is given by:

$$\frac{M}{V} = -\frac{1}{4\pi} \frac{1}{1-d} H.$$

Calculation after Crabtree<sup>20</sup> for thin cylinders of 3 mm diameter, 240, 80, and 30nm height gave the geometry factors  $1/(1-d) \sim 3600$ , 7700, and 24000, respectively.

### III. RESULTS AND DISCUSSION

Measurements on our pure Nb films with various thicknesses have not found any PME signal. Apparently the surface property of our films is not much different from the bulk. On the contrary, when the surfaces of the Nb films are covered by Co layers, PME was found when Nb thickness is larger than the penetration depth.

Fig. 1 shows examples of field-cooled and zero-field-cooled magnetic response to perpendicular magnetic field versus temperature. Data were taken while warming. Clear paramagnetic signals were seen for these samples with Nb thickness 240 or 80 nm. The 80 nm sample showed larger signal than the 240 nm one due to the demagnetization factor. When normalized to the ZFC susceptibilities, the signals correspond to 0.6 and 0.55 percents. However, several samples with 30 nm thick Nb showed only Meissner effect. That is, PME was seen when Nb thickness was no less than the penetration depth. Since all samples have the same total Nb thickness, this behavior was not due to difference in S volume. Fig. 2 depicts a model for the occurrence of PME after Koshelev and Larkin.<sup>13</sup> Since the free surface on the sides has higher  $T_C$ , superconductivity is established there first. Large amount of flux can be trapped inside the sample. The diamagnetic shielding current  $I_S$  and paramagnetic pinning current  $I_P$  are then functions of the sample geometry. For our thin plate orthogonal to the field, competition between the two currents results in the PME.

To be sure these PME signals were not due to the expelled magnetic flux from Meissner state of Nb layers enhancing the moments of the Co layers, we have studied the hysteresis loops at 10K with field perpendicular to the surface carefully. All our samples have easy axis for Co layers lying in the plane with coercive fields less than 80Oe. The perpendicular direction is a hard direction with much larger coercive field. The magnetic state at zero field depends on the history of the sample and can be manipulated by performing field minor loops to any point below remanence. The inset of Fig. 3 shows the hysteresis loop and two initial magnetization curves of the 240nm Nb sample. The slopes of the initial magnetization

curve, i.e. the susceptibilities, indicate how easily the magnetic moments can be rotated out of the in-plane easy axis direction. These slopes for three samples are shown in Fig. 3. One can see that different Co thickness did not show much different  $dM/dH$  value at low field. The slope exhibited large change only when field was at 90 Oe or larger. Thus we rule out the possibility of the expelled flux lines when the Nb layers go into S state as the major contribution of the paramagnetic signals.

Since the observed paramagnetic signals were indeed from the PME, we performed calculations for a complete Bean state following Ref. 13. As an approximation, we use Eq. (13) in Ref. 13 for a disk sample with radius  $R$  and thickness  $d$ . Because the presence of Co, moving magnetic flux around costs energy. Thus we assume a case of weak flux compression, i.e., the shielding current ( $I_S$  in Fig. 2) flows only in the region  $\lambda$  of several penetration depths near the free surface. The paramagnetic signal normalized to the complete Meissner signal is<sup>13</sup>

$$\frac{M}{M_M} = 1.08 \left[ -(1-f) + \frac{\lambda}{R} \left( \ln \frac{R}{\lambda} - 0.96 \right) \right]$$

where  $f$  is the fraction of trapped flux. We obtained that the two samples in Fig. 1 both had  $f$  around 99.5%. If  $\lambda$  is as long as 10 micron,  $f$  is about 97%. In a weak compression case,  $f$  must be larger than 95% and the PME is small. In a strong compression case, the PME signal ranges between 27% and 0% for  $f$  ranges from 100% to 80%. For the dependence of resulting PME signals on  $\lambda$  and  $f$ , see Fig. 4 in Ref. 13. The large  $f$  in our case can be attributed to the presence of Co helps to trap flux and to reduce interface  $T_C$ . The absence of PME in samples with 30nm thick Nb can be explained by the critical current density,  $j_C$ , and how fast  $j_C$  increases with decreasing temperature. The critical current enters the above equation through  $f$ . The pinning current density required to maintain the compressed flux must not exceed  $j_C$ , otherwise the flux will move out of the sample and the PME cannot be achieved. Fig. 4 shows our data on  $j_C$  versus temperature measured on 2 micron wide, 40 micron long samples. The 240 nm thick Nb sample has a value and shape close to the bulk behavior. The  $j_C$  of the 30 nm sample is about 20% of the 240 nm one close to  $T_C$ , that is, the slope of  $j_C$  increasing with decreasing temperature differs by 5 times. Comparing the estimated pinning currents and the  $j_C$ 's, we found  $j_C$  is more than two orders of magnitude larger in the 240 nm thick Nb sample. In the 30 nm Nb sample, the two currents are the same order. Thus, in the 30 nm sample, when temperature decreases

from  $T_C$ , the increase of  $j_C$  is insufficient to support the trapped flux. Paramagnetic flux has to move out of the sample and no PME can be formed. We infer that the penetration depth of S materials is a critical length due to the reduction of critical current density and of the slope of  $j_C$  increasing with decreasing temperature. Only when S layer thickness is larger than the penetration depth, could the PME be found.

The role of proximity effect is essential in this study. It suppresses the interface  $T_C$  to allow the free surface to go into superconducting state first while the sample is slowly cooling down. The critical current density near the interface is strongly reduced due to the fringe fields of strong magnetic Co layers. A detail discussion of the proximity effect between Co and Nb will be published elsewhere.<sup>18</sup> Here we discuss briefly the behavior of the related samples. From upper critical field measurements, we found the Ginzburg-Landau superconducting coherence lengths at zero degree were 12 nm to 13 nm parallel to the plane and 9 nm to 10 nm perpendicular to the plane. Close to  $T_C$ , the Ginzburg-Landau coherence length is inversely proportional to  $(T_C - T)^{1/2}$ . When Nb is 30 nm thick, the coherence length and penetration depth just below  $T_C$  are as larger as the thickness. The fringe field of Co affects the thick Nb films only at the interfaces, but reduces the critical current for 30 nm Nb thickness a lot. Thus, the required amount of trapped flux in the model of Koshelev and Larkin cannot be fulfilled for 30 nm thick Nb samples.

#### IV. SUMMARY

Paramagnetic Meissner effect was studied for superconducting thin films with thickness in the regime close to penetration depth. We have shown clear evidence that Co/Nb/Co trilayers and multilayers showed PME when Nb thickness is no less than its penetration depth. The total magnetic moment is not linearly additive of each layer's due to the trapped flux and induced current are functions of sample geometry. This gives us the possibility to manipulate flux lines in engineered superconductor/ferromagnet structures.

---

<sup>1</sup> W. Braunisch, N. Knauf, V. Kataev, S. Neuhausen, A. Grütz, B. Roden, D. Khomskii, and D. Wohlleben, Phys. Rev. Letts. **68**, 1908 (1992).

- <sup>2</sup> D. J. Thompson, M. S. M. Minhaj, L. E. Wenger, and J. T. Chen, Phys. Rev. Lett. **75**, 529 (1995).
- <sup>3</sup> P. Kostic, B. Veal, A. P. Paulikas, U. Welp, V. R. Todt, C. Gu, U. Geiser, J. M. Williams, K. D. Carlson, and R. A. Klemm, Phys. Rev. B **53**, 791 (1996).
- <sup>4</sup> J. J. Hauser, H. C. Theuerer, and N. R. Werthamer, Phys. Rev. **142**, 118 (1966).
- <sup>5</sup> L. Lazar, K. Westerholt, H. Zable, L. R. Tagirov, Yu. V. Goryunov, N. N. Garif'yanov, and I. A. Garifullin, Phys. Rev. B **61**, 3711 (2000).
- <sup>6</sup> G. Verbanck, C. D. Potter, V. Metlushko, R. Schad, P. Belien, V. V. Moschalkov, Y. Bruynseraede, Phys. Rev. B **57**, 6029 (1998).
- <sup>7</sup> I. Banerjee and I. K. Schuller, J. Low Temp. Phys. **54**, 501 (1984).
- <sup>8</sup> P. Svelindh, K. Niskanen, P. Norling, P. Nordblad, L. Lundgren, B. Lönnberg, and T. Lundström, Physica C **162-164**, 1365 (1989).
- <sup>9</sup> L. Pust, L. E. Wenger, and M. R. Koblishka, Phys. Rev. B **58**, 14191 (1998).
- <sup>10</sup> A. Terentiev, D. B. Watkins, L. E. De Long, D. J. Morgan, and J. B. Ketterson, Phys. Rev. B **60**, R761 (1999).
- <sup>11</sup> A. K. Geim, S. V. Dubonos, J. G. S. Lok, M. Henini, and J. C. Maan, Nature **396**, 144 (1998).
- <sup>12</sup> M. Sigrist and T. M. Rice, Rev. Mod. Phys. **67**, 503 (1995).
- <sup>13</sup> A. E. Koshelev, and A. I. Larkin, Phys. Rev. B **52**, 13559 (1995).
- <sup>14</sup> V. V. Moshchalkov, X. G. Qiu, and V. Bruyndoncx, Phys. Rev. B **55**, 11793 (1997).
- <sup>15</sup> S. F. Lee, T. M. Chuang, S. Y. Huang, W. L. Chang, Y. D. Yao, J. Appl. Phys. **89**, 7493 (2001).
- <sup>16</sup> S. F. Lee, Y. Liou, Y. D. Yao, W. T. Shih, and C. Yu, J. Appl. Phys. **87**, 5564 (2000).
- <sup>17</sup> Th. Muhge, K. Westerholt, H. Zabel, N. N. Garif'yanov, Yu. V. Goryunov, I. A. Garifullin, and G. G. Khaliullin, Phys. Rev. B **55**, 8945 (1997); **57**, 5071 (1998).
- <sup>18</sup> To be published.
- <sup>19</sup> F. J. Blunt, A. R. Perry, A. M. Campbell and R. S. Liu, Physica C **175**, 539 (1991).
- <sup>20</sup> G. W. Crabtree, Phys. Rev. B **16**, 1117 (1977).

## Figure Captions

Fig. 1. PME moment versus temperature of two samples: Co(15nm)/Nb(240nm)/Co(15nm) in circles and [Co(7.5nm)/Nb(80nm)] $\times$ 3/Co(7.5nm) in triangles. Samples were kept stationary and field cooled at  $H=0.57\text{Oe}$ . Measurements were made with a warming rate of  $0.05\text{K/Min}$ . The normalized zero-field-cooled and field-cooled susceptibilities are shown in the inset with solid and dash lines. PME susceptibilities are 0.60 and 0.55 percents, respectively.

Fig. 2. Schematic cross-section of a Co/Nb/Co trilayer. The free surface has higher  $T_C$  and superconducts first. Competition between diamagnetic shielding current,  $I_S$ , and paramagnetic pinning current,  $I_P$ , results in PME due to the thin plate orthogonal to field geometry. Drawing is not to scale.

Fig. 3. Slope of the initial magnetization curve of three samples: [Co(15nm)/Nb(240nm)] $\times$ 5/Co(15nm) in squares, [Co(7.5nm)/Nb(80nm)] $\times$ 15/Co(7.5nm) in circles, and [Co(2.2nm)/Nb(30nm)] $\times$ 40/Co(2.2nm) in triangles with perpendicular field measured at 10K. The first two samples do not have particular high value than the third one. This indicates that increased Co moment by repelled flux while Nb layers go into superconducting state is not responsible for the PME signals in Fig. 1. The inset shows the hysteresis loop of the first (Nb240nm) sample with two initial magnetization curves in square. The zero field states were reached by performing field minor loops. Notice the curves are close to linear at low field and the slopes are similar.

Fig. 4. Critical current density versus reduced temperature for Nb thicknesses 240 and 30 nm sandwiched between Co layers.

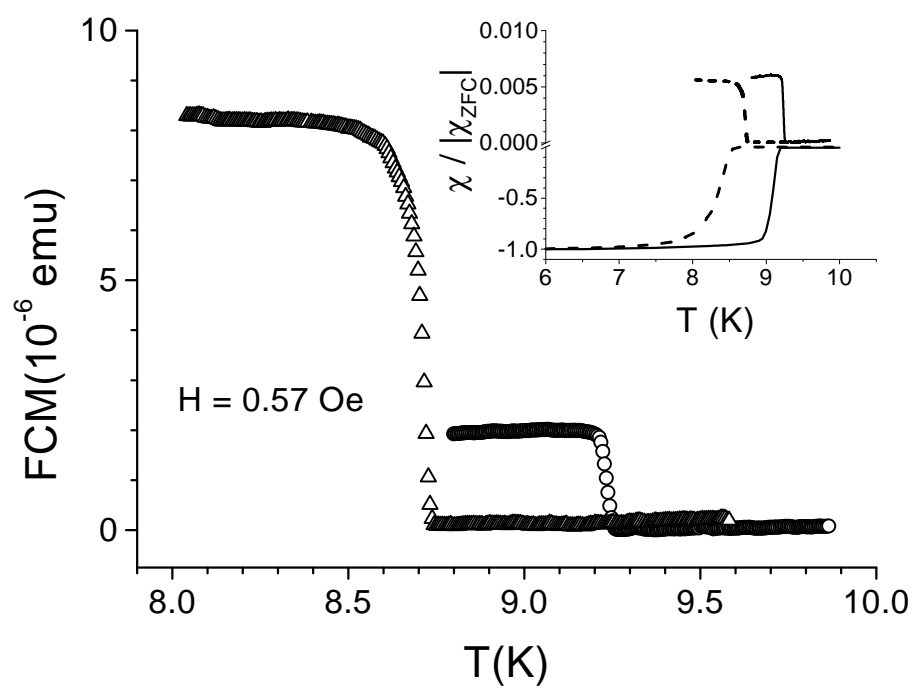


Figure 1 S. F. Lee et al.

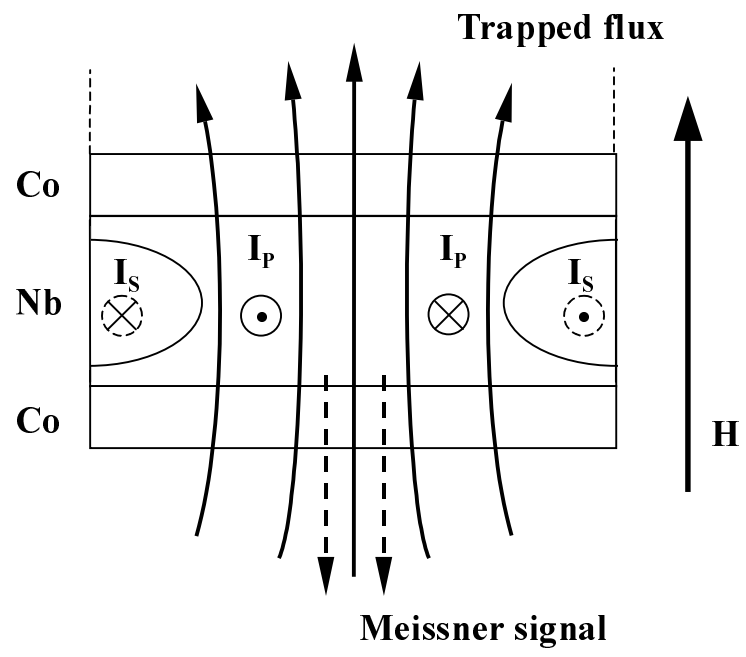


Figure 2 S. F. Lee et al.

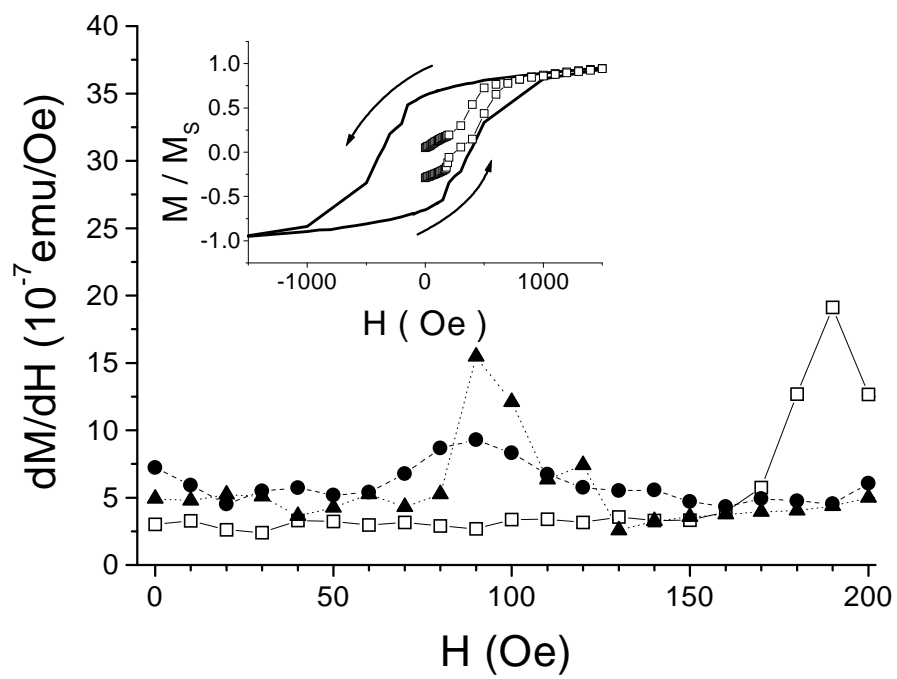


Figure 3 S. F. Lee et al.

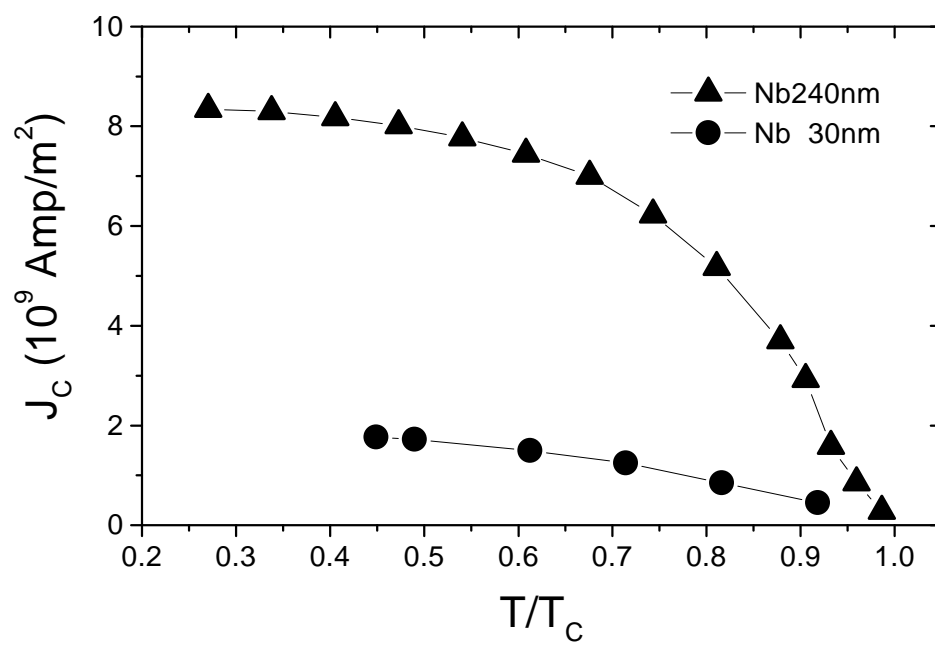


Figure 4 S. F. Lee et al.